Reproducibility of Myocardial T_1 and T_2 Relaxation Time Measurement Using Slice-Interleaved T_1 and T_2 Mapping Sequences

Steven Bellm, MD,[1] Tamer A. Basha, PhD,[1] Ravi V. Shah, MD,[1] Venkatesh L. Murthy, PhD,[2] Charlene Liew, MD,[1] Maxine Tang, MS,[1] Long H. Ngo, PhD,[1] Warren J. Manning, MD,[1,3] and Reza Nezafat, PhD[1]*

Purpose: To assess measurement reproducibility and image quality of myocardial T_1 and T_2 maps using free-breathing slice-interleaved T_1 and T_2 mapping sequences at 1.5 Tesla (T).

Materials and Methods: Eleven healthy subjects (33 ± 16 years; 6 males) underwent a slice-interleaved T_1 and T_2 mapping test/retest cardiac MR study at 1.5T on 2 days. For each day, subjects were imaged in two sessions with removal out of the magnet and repositioning before the subsequent session. We studied measurement reproducibility as well as the required sample size for sufficient statistical power to detect a predefined change in T_1 and T_2. In a separate prospective study, we assessed T_1 and T_2 map image quality in 241 patients (54 ± 15 years; 73 women) with known/suspected cardiovascular disease referred for clinical cardiac MR. A subjective quality score was used to assess a segment-based image quality.

Results: In the healthy cohort, the slice-interleaved T_1 measurements were highly reproducible, with global coefficients of variation (CVs) of 2.4% between subjects, 2.1% between days, and 1.7% between sessions. Slice-interleaved T_2 mapping sequences provided similar reproducibility with global CVs of 7.2% between subjects, 6.3% between days, and 5.0 between sessions. A lower variability resulted in a reduction of the required number of subjects to achieve a certain statistical power when compared with other T_1 mapping sequences. In the subjective image quality assessment, >80% of myocardial segments had interpretable data.

Conclusion: Slice-interleaved T_1 and T_2 mapping sequences yield highly reproducible T_1 and T_2 measurements with >80% of interpretable myocardial segments.

J. MAGN. RESON. IMAGING 2016;44:1159–1167.

Myocardial interstitial diffuse fibrosis, inflammation, and edema are present in many diseases such as cardiomyopathy,[1] hypertension,[2] aortic regurgitation,[3] and myocarditis.[4] Therefore, noninvasive assessment of myocardial tissue composition of fibrosis, edema, and inflammation may have an important clinical impact in diagnosis, prognosis, and monitoring of therapy. Myocardial tissue relaxometry has been emerging as a clinically powerful tool to characterize myocardial tissue composition.[5] Myocardial T_1 relaxation time changes in the presence of interstitial diffuse fibrosis and can be assessed using native T_1 and extracellular volume (ECV) mapping.[6,7] Changes in myocardial T_2 relaxation time in the presence of edema and inflammation can also be quantitatively measured using myocardial T_2 mapping.[4,8,9]

Over the past decade, there have been numerous advances in cardiac MR sequences for myocardial T_1 and T_2 mapping.[10–23] T_1 mapping sequences sample the magnetization recovery curve to enable estimation of T_1 recovery by voxel-wise curve fitting. The modified Look-Locker

View this article online at wileyonlinelibrary.com. DOI: 10.1002/jmri.25255

Received Jan 13, 2016, Accepted for publication Mar 9, 2016.

*Address reprint requests to: R.N., Beth Israel Deaconess Medical Center, 330 Brookline Avenue, Boston, MA, 02215. E-mail: rnezafat@bidmc.harvard.edu

From the [1]Department of Medicine (Cardiovascular Division), Beth Israel Deaconess Medical Center, Harvard Medical School, Boston, Massachusetts, USA; [2]Department of Medicine (Cardiovascular Division), University of Michigan, Ann Arbor, Michigan, USA; and [3]Department of Radiology, Beth Israel Deaconess Medical Center, Harvard Medical School, Boston, Massachusetts, USA.

inversion recovery (MOLLI)[13] and shortened MOLLI (ShMOLLI)[14] sequences are widely used for myocardial T_1 mapping. Saturation recovery based sequences, such as modified Look-Locker acquisition using saturation recovery,[15] SAturation recovery single-SHot Acquisition (SASHA),[16] and saturation method using adaptive recovery times for cardiac T_1 mapping ($SMART_1Map$) sequence,[17] have also been investigated. These sequences allow more accurate T_1 measurements, however, with a penalty in precision and reproducibility.[18]

A combination saturation and inversion recovery based sequence, i.e., saturation pulse prepared heart rate independent inversion recovery (SAPPHIRE)[19] sequence has also been investigated. A free-breathing slice-interleaved T_1 mapping sequence (STONE)[20] has been recently proposed that enables T_1 measurements of five short-axis slices over the entire left ventricle in a free-breathing 95 second scan. This sequence is based on interleaving data acquisition for different slices during the recovery time of adjacent slices. A longer recovery of spins for each individual slice results in improved accuracy and precision.[20]

Myocardial T_2 mapping is often performed by acquiring multiple T_2 prepared (T_2prep) balanced steady-state free-precession images, each followed by rest periods of magnetization recovery, and estimating the voxel-wise T_2 values.[21] This is often performed with one breathhold for each slice. Three-dimensional (3D) myocardial T_2 mapping is an alternative to 2D T_2 mapping so as to improve spatial resolution and coverage of myocardial T_2 mapping.[22] A slice-interleaved T_2 mapping sequence was recently developed by implementing a slice-selective T_2Prep to interleave the data acquisition for different slices in subsequent heartbeats.[23] This free-breathing slice-interleaved T_2 mapping sequence allows T_2 measurements of five parallel left ventricular (LV) short-axis slices with similar precision as a single-slice T_2 mapping sequence, but with a fourfold reduction in acquisition time.[23]

In recent years, there has been interest in applying regional myocardial T_1 and T_2 mapping as imaging markers of disease progression or response to a specific therapy/intervention. Knowledge of measurement reproducibility is important to distinguish between changes that could be attributable to measurement variability and those that are the result of disease progression or therapeutic intervention. Furthermore, to justify the sample size for the achievement of a specific statistical power, the reproducibility of these measurements needs to be known. Finally, image quality assessment should be performed to take into account the percentage of nondiagnostic images acquired with these sequences. To address these challenges, we sought to: (1) investigate reproducibility of recently developed free-breathing slice-interleaved T_1 and T_2 mapping sequences in a cohort of healthy adult subjects by performing a comprehensive test/re-test study; (2) investigate the required sample size to achieve certain statistical power for detection of a predefined change in native T_1 or T_2; and (3) assess overall T_1 and T_2 map image quality using the slice-interleaved T_1 and T_2 mapping sequences in patients with known or suspected cardiovascular disease referred for clinical cardiac MR.

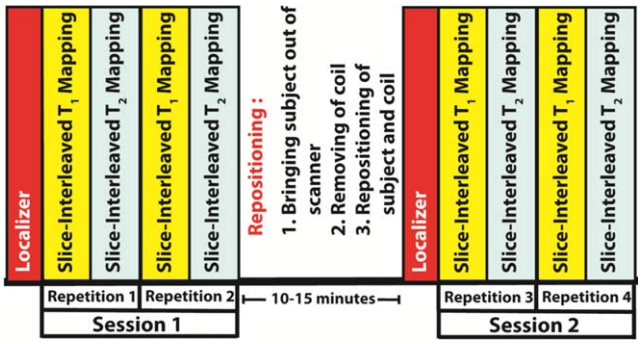

FIGURE 1: Study protocol: Healthy subjects (n = 11) underwent MR imaging to assess acquisition reproducibility between days, sessions, and repetitions. The study protocol was identical in both days. Each sequence was repeated twice per session. Between two different sessions, subjects were taken out of the scanner, and the 32-channel phased array coil was repositioned before starting the next session.

Materials and Methods

All imaging was performed on a 1.5T Philips Achieva (Philips Healthcare, Best, The Netherlands) MRI system using a 32-channel cardiac coil. The study was Health Insurance Portability and Accountability Act (HIPAA) compliant. The imaging protocol was approved by our institutional review board and written informed consent was obtained from each participant prior to scanning.

Reproducibility Assessment

In a prospective study, we recruited 11 healthy adult subjects (33 ± 16 years; 6 men) without contraindications for cardiac MR to participate in a 2-day test/retest study using an imaging protocol shown in Figure 1. Each subject underwent cardiac MR imaging on two different days (between-day reproducibility) with the identical imaging protocol. After image localization, the subjects were imaged using slice-interleaved T_1 and T_2 mapping sequences in five left ventricular short-axis view slices over the entire ventricle (from apex to base). Each sequence was repeated twice (within-session reproducibility). Following completion of the first imaging session, subjects were taken out of the scanner for a 10- to 15-min break with removal of the coil. Subsequently, subjects were scanned again, after image localization, for a second session (between-session reproducibility) with two repetitions per sequence.

T_1 mapping was performed using slice-interleaved T_1 mapping sequence with the following parameters: five short-axis slices, in-plane resolution= 2.1 × 2.1 mm^2, slice thickness = 8 mm, slice gap = 4 mm, field-of-view = 320 × 320 mm^2, repetition time/echo time/alpha (TR/TE/α) = 2.8 ms / 1.38 ms / 70°, SENSE-rate = 2, linear ordering, 10 linear ramp-up pulses and acquisition window = 218.8 ms, bandwidth = 1879.7 Hz/pixel.

T_2 mapping was performed using slice-interleaved T_2 mapping sequence with the following parameters: five short-axis slices, in-plane resolution = 2.1 × 2.1 mm^2, slice thickness = 8 mm, slice gap = 4 mm, field-of-view = 320 × 320 mm^2, TR/TE/α = 2.8 ms / 1.38 ms / 55°, SENSE-rate = 2.3, linear ordering, 10 linear ramp-up pulses and acquisition window = 191.1 ms, bandwidth = 1879 Hz/pixel. Images for both T_1 and T_2 mapping were acquired during free-breathing with slice tracking. A two-dimensional pencil beam navigator was positioned at the dome of the right hemidiaphragm to monitor the diaphragmatic motion and to correct the slice position during imaging. Slice tracking was used without any respiratory gating.

Impacts on Sample Size Calculation

Using T_1 and T_2 measurements from our healthy subject cohort, we performed statistical analyses to determine the number of subjects that are needed to achieve a certain power for detection of specific changes in T_1 and T_2. For sample size assessment, we compared the results of slice-interleaved T_1 with T_1 measured using MOLLI and ShMOLLI. As we did not directly acquire data using MOLLI or ShMOLLI, this variability was extracted from a previously published study.[18] Correspondingly, we compared the results of slice-interleaved T_2 with T_2 measured by using single-slice T_2 mapping sequence. The data for the single-slice T_2 sequence were acquired in the same sessions as the slice-interleaved sequences with our 11 healthy subjects using the identical study design. The sequence was performed by using the following parameters: five short-axis slices, in-plane resolution = 2.1 × 2.1 mm^2, slice thickness = 8 mm, slice gap = 4 mm, field-of-view = 320 × 320 mm^2, TR/TE/α = 2.9 ms / 1.43 ms / 55°, SENSE-rate = 2.3, linear ordering, 10 linear ramp-up pulses and acquisition window = 197.3 ms, bandwidth = 1879 Hz/pixel. T_1 and T_2 measurements from the mid-LV slice were used for all calculations in the sample size analysis.

Image Quality Assessment

For patient image quality assessment, we prospectively enrolled 246 patients (54 ± 15 years; 73 women) with known or suspected cardiovascular disease referred for a clinical cardiac MR exam over a period of 15 months. The imaging protocol was approved by our institutional review board and written informed consent was obtained from each participant before each examination for the addition of T_1 and T_2 mapping sequences to their standard clinical exam. Slice-interleaved T_1 and T_2 mapping sequences were acquired in addition to their clinically indicated imaging protocol. Imaging parameters were similar to the healthy subject study. The slice-interleaved T_1 mapping sequence had the following imaging parameters: five short-axis slices, in-plane resolution = 2.1 × 2.1 mm^2, slice thickness = 8 mm, slice gap = 4 mm, field-of-view = 360 × 352 mm^2, TR/TE/α = 2.8 ms / 1.39 ms / 70°, SENSE-rate = 2, linear ordering, 10 linear ramp-up pulses and acquisition window = 239.8 ms, bandwidth = 1845 Hz/pixel. The slice-interleaved T_2 mapping sequence had the following parameters: five short-axis slices, in-plane resolution = 2 × 2 mm^2, slice thickness = 8 mm, slice gap = 4 mm, field-of-view = 320 × 320 mm^2, TR/TE/α = 2.8 ms / 1.41 ms / 55°, SENSE-rate = 2.5, linear ordering, 10 linear ramp-up pulses and acquisition window = 188.7 ms, bandwidth = 1785.7 Hz/pixel. Because of limited availability of scan time and the heterogeneity of our patient cohorts, no reproducibility assessments were performed in this cohort.

Data Analysis

REPRODUCIBILITY STUDY. All images were transferred to a separate workstation for analysis. T_1 and T_2 mapping of each scan were estimated by voxel-wise curve fitting of the signal after motion correction. In-plane motion between different images of T_1 and T_2 maps were corrected using image registration by a nonrigid image registration algorithm.[24] T_1 values were estimated by fitting the recovery curve to a two-parameter and T_2 values to a three-parameter fitting model.[25] The endocardial and epicardial contours of the LV myocardium were manually outlined. The anterior right ventricular (RV) insertion point was marked as a point of reference to generate a 26-segment model of five slices over the entire left ventricle from apex to base.

Additionally, a mean T_1/T_2 estimate was generated for each of the five single slices and for the entire ventricle. Artifacts were excluded by manually drawn regions of interest (ROIs) and any segment with visual artifacts after segment analysis was excluded from the analysis. A second experienced reader analyzed T_1 and T_2 measurements for one repetition in all subjects, which was compared with results of the corresponding repetition of the first reader, to assess interobserver agreement by using intraclass correlation coefficient (ICC) analysis. Intraobserver agreement was assessed by using ICC analysis for two corresponding repetitions of each subject analyzed by one reader. Continuous values were presented as mean ± standard deviation (SD). The Shapiro-Wilk test was used to assess for normal distribution. CV analysis was generated to assess variability between subjects, days and sessions and was visualized by box plots. Significance was considered as *P*-value less than 0.05. Data analysis was performed with SPSS software (SPSS, Version 17, Inc., Chicago, IL) and Matlab software (The MathWorks Inc., Natick, MA).

IMPACTS ON SAMPLE SIZE CALCULATION. A linear mixed effects model was used to calculate variance estimations for the effect of volunteers, days, sessions, repetitions, and remaining unspecified factors (i.e., heart rate, etc.). For this model, imaging day is nested within subjects, session is nested within day, and repetition is nested within session. This analysis provides individual variances for each individual factor, a pooled variance and pooled standard deviation for each T_1 (slice-interleaved/MOLLI/ShMOLLI) and T_2 (slice-interleaved/single-slice) mapping sequence. The sample size assessment was performed for 90%, 85%, and 80% power groups for detection of different changes in T_1 and T_2 values at a type 1 error of 0.05.

IMAGE QUALITY ASSESSMENT. Subjective image quality was assessed by two readers (S.B. with 2 years of experience and C.L. with 6 years of experience) using a 26-segment LV model. The LV was divided into five short-axis slices perpendicular to the longitudinal axis of the heart. This leads to five circular sections of the LV-myocardium (basal, three mid-ventricular and apical slices). Only slices with complete circular section of the LV were included.

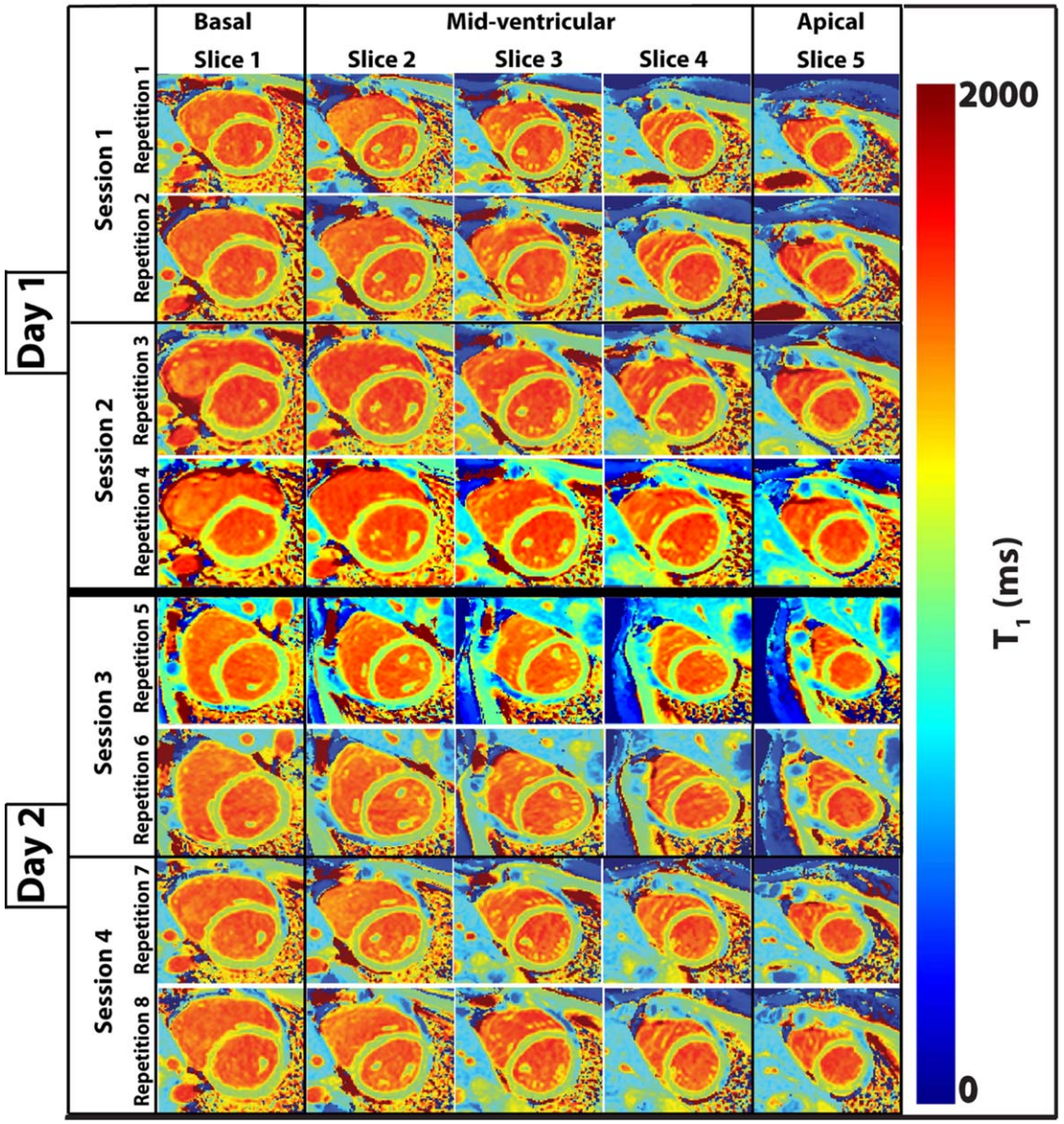

FIGURE 2: Example T_1 maps acquired with the STONE sequence.

Each of the three most basal sections were divided into six segments of 60° each. Each of the two most apical slices were divided into four segments of 90° each. Segments were evaluated independently by two readers. A score of 1 was given if the segment was of acceptable image quality for analysis, defined in this study as having at least a 5 × 5 pixel ROI not affected by artifact. Otherwise, a score of 0 was given to this segment. Interobserver agreement for both slice-interleaved T_1 and T_2 maps were calculated.

Results

Reproducibility Study

Figure 2 shows example T_1 mapping images of five short-axis LV slices for the slice-interleaved T_1 sequence with eight repetitions (2 days × two sessions × two repetitions). All five slices of the eight repetitions appear with homogeneous quality and without artifacts. Figure 3 is an example of eight repetitions of T_2 mapping of five LV slices for slice-interleaved T_2 sequence. All slices in all repetitions of this subject show homogeneous quality and are without artifacts. Figure 4 shows individual and group global T_1 and T_2 estimates among all 11 healthy subjects at each repetition. Each sequence was repeated twice per session. There were two sessions on each of the 2 days. The results including SDs for both sequences appeared very similar between different repetitions, sessions and days. The global mean T_1 time for slice-interleaved T_1 was 1063 ± 22 ms and the global mean T_2 time for slice-interleaved T_2 was 48 ± 5 ms. Figure 5 shows global T_1 and T_2 estimates for each of the five slices among all repetitions and subjects. The slices within each sequence showed similar global T_1 and T_2 estimates. Segments compromised by severe artifacts were

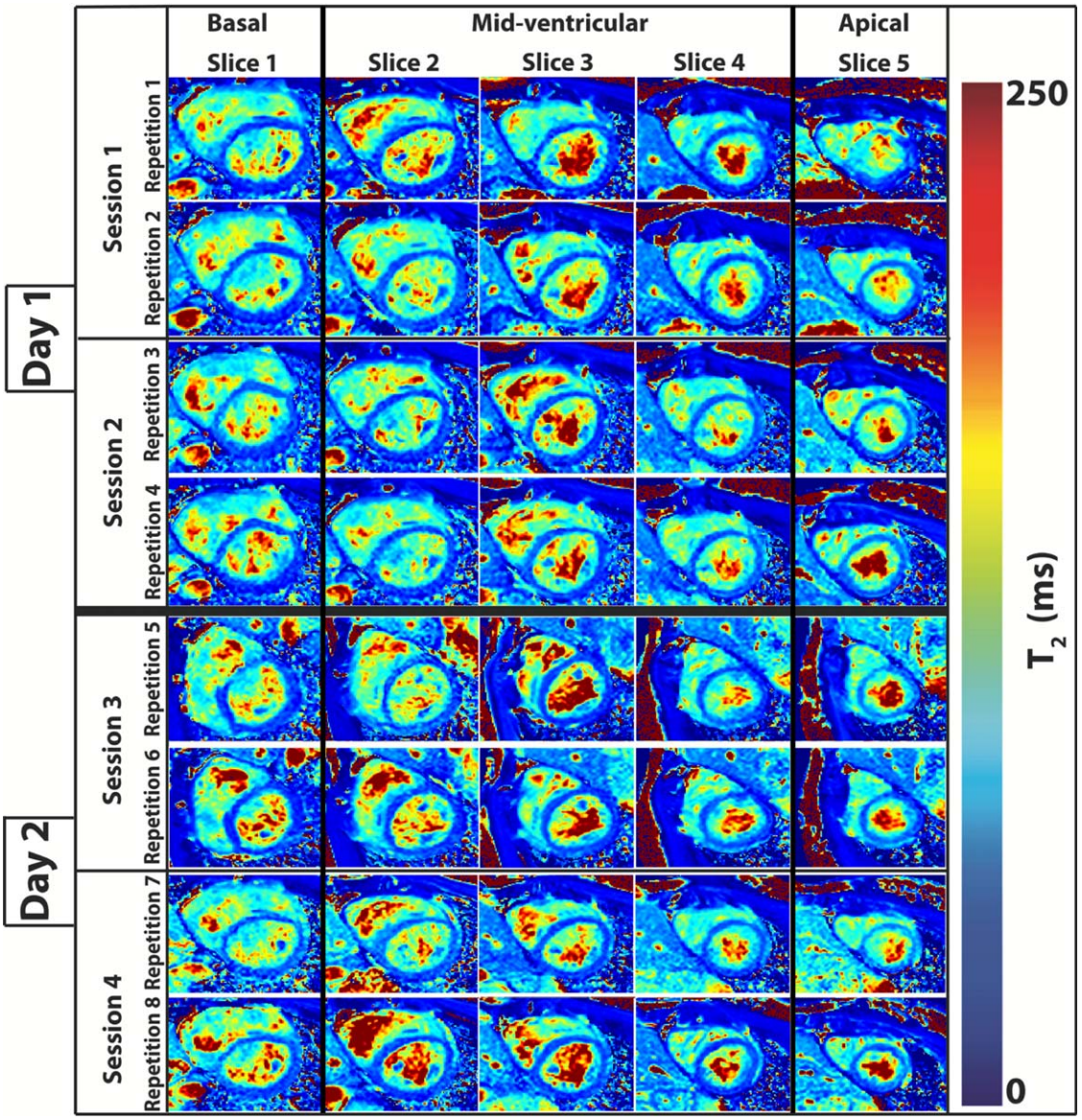

FIGURE 3: Example T_2 maps acquired with the free-breathing slice-interleaved T_2 mapping sequence.

excluded (T_1: 5.6% and T_2: 16.3%). Slice-interleaved T_2 showed a higher tendency for motion artifacts than slice-interleaved T_1.

The CV analysis between different subjects, days, and sessions and for both sequences showed a high reproducibility with global CVs of < 5% between days, sessions and subjects (Fig. 6). The CV analysis for individual slices showed a low variability for slice-interleaved T_1 (global CV per slices: slice 1 = 2.7%; slice 2 = 2.8%; slice 3 = 3.2%; slice 4 = 3.1%; slice 5 = 3.7%) as well as slice-interleaved T_2 (global CV per slices: slice 1 = 12.5%; slice 2 = 11.5%; slice 3 = 8.8%; slice 4 = 9.4%; slice 5 = 8.3%). The most apical and most basal slices (slice 1 and slice 5) showed similar reproducibility as compared to the three mid-ventricular slices (slices 2–4) in both sequences after exclusion of segments with severe artifacts.

The interobserver agreement for slice-interleaved T_1 sequence showed an excellent agreement with an ICC of 0.86 (95% confidence interval: 0.13 to 0.97). The interobserver agreement for slice-interleaved T_2 sequence was very strong with an ICC of 0.75 (95% confidence interval: 0.17–0.93). The intraobserver agreement for slice-interleaved T_1 sequence showed an excellent agreement with an ICC of 0.87 (95% confidence interval: 0.35–0.97) and the intraobserver agreement for slice-interleaved T_2 sequence was very strong with an ICC of 0.77 (95% confidence interval: 0.12–0.94).

Impacts on Sample Size Calculation

Figure 7 shows the required sample size to detect changes in T_1 measured using STONE, MOLLI, and ShMOLLI at three different statistical power levels (>90%, >85%,

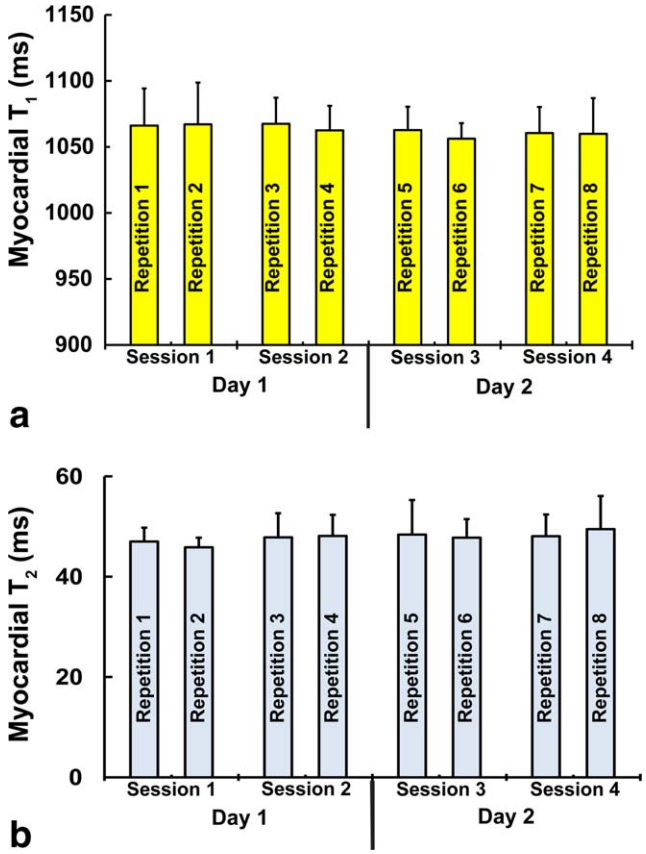

FIGURE 4: Mean ± standard deviation (among different subjects) of global myocardial T_1 (A) and T_2 (B) measurements for different repetitions.

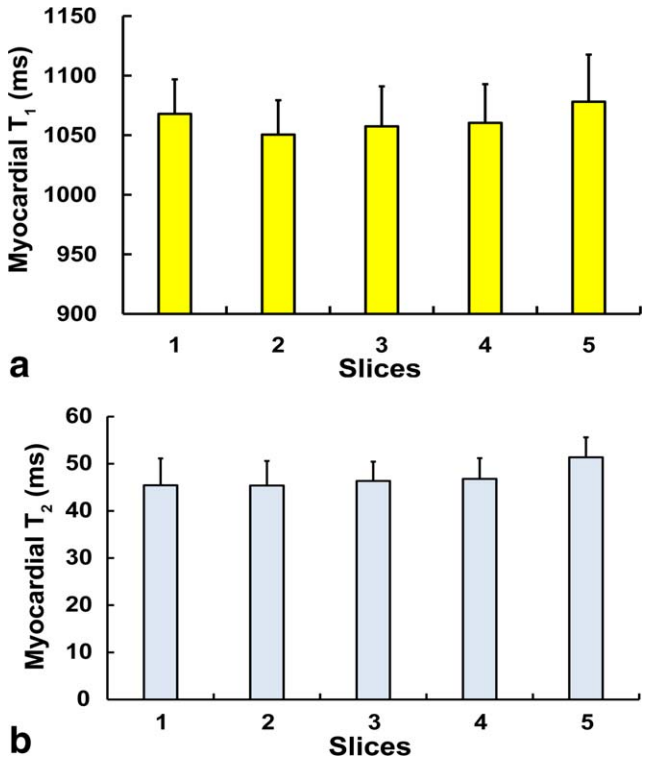

FIGURE 5: Mean ± standard deviation (among different subjects) of global myocardial T_1 (A) and T_2 (B) estimates for different slices (basal: slice 1, mid-ventricular: slices 2–4, and apical: slice 5).

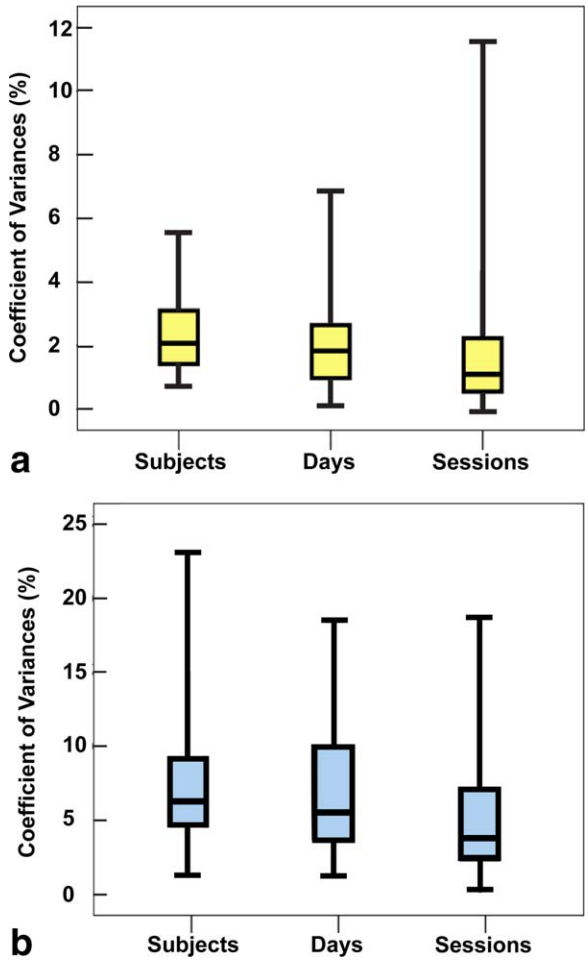

FIGURE 6: Coefficient of variation analysis for T_1 (A) and T_2 (B) mapping sequences to assess the variability between different subjects, days and sessions.

>80%). The required sample size for detection of a specific T_1 difference is smaller for STONE than for MOLLI and ShMOLLI. Figure 8 shows the required sample size to detect changes in T_2 measured by using slice-interleaved T_2 and single-slice T_2 mapping sequences at three different statistical power levels (>90%, >85%, >80%). For both T_2 sequences, the required sample sizes are very similar for detection of T_2 differences. For detection of T_2 differences of ≤10 ms, single-slice T_2 requires fewer subjects than slice-interleaved T_2.

Image Quality Assessment

Five patients were excluded from analysis due to incorrect positioning of the slices and/or reconstruction error. Figure 9 shows the subjective image score (averaged between the two readers) for each of the 26 T_1 and T_2 map segment. The lowest scores consistently seen on both T_1 and T_2 maps were at the most basal and most apical slices (slices one and five, respectively) and adjacent to the RV insertion points into the interventricular septum. The mean visual quality scores for the most basal slices were 0.81 ± 0.04 and 0.81 ± 0.04 for T_1 and T_2 maps, respectively. The

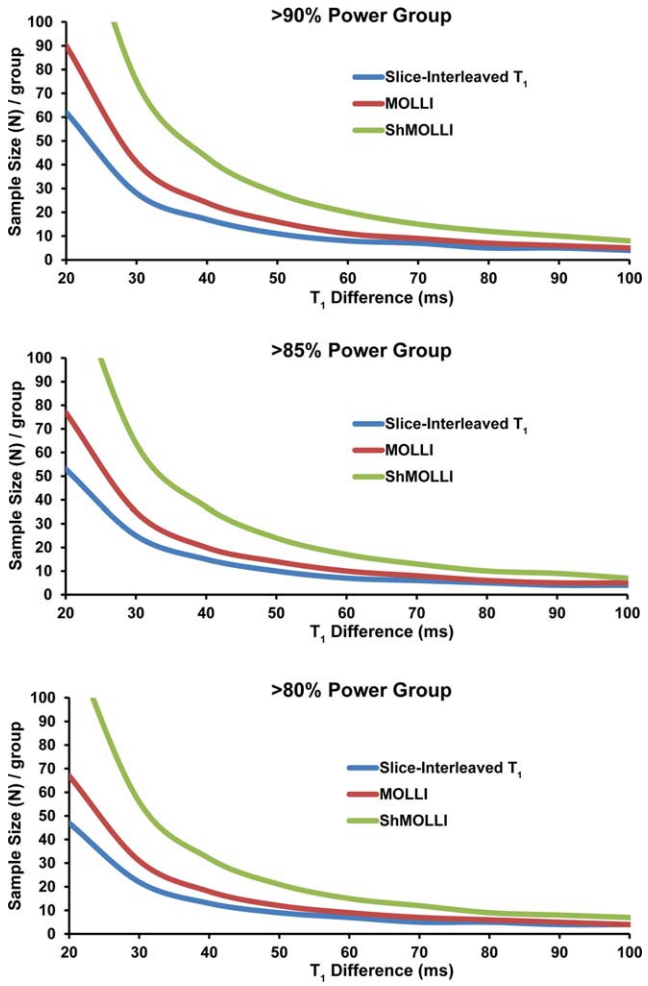

FIGURE 7: Assessment of required sample size for detection of corresponding T_1 differences in STONE, MOLLI, and ShMOLLI mapping sequences for three different power levels (>90%, >85%, >80%; $\alpha = 0.05$).

mean visual quality scores for the most apical slices were 0.61 ± 0.03 and 0.76 ± 0.03 for T_1 and T_2 maps, respectively. The septal wall segments demonstrated the best scores in both T_1 and T_2 maps, with mean visual quality scores of 0.85 ± 0.09 and 0.84 ± 0.04 for T_1 and T_2 maps, respectively. Using the Wilcoxon signed-rank test, the mean score differences between basal and septal as well as apical and septal segments were significantly different ($P < 0.001$) for T_1 and T_2 maps, respectively.

The interobserver agreement for visual quality scores of slice-interleaved T_1 maps showed strong agreement with an ICC of 0.74 (95% confidence interval: 0.64–0.81). The interobserver agreement for quality scores of slice-interleaved T_2 sequence was moderate to good with an ICC of 0.60 (95% confidence interval: 0.35–0.74).

Discussion

In this prospective study examining T_1 and T_2 reproducibility with slice-interleaved T_1 and T_2 mapping sequences in healthy subjects and subjective image quality in patients with known or suspected cardiovascular disease, we found that these two free-breathing sequences provide excellent reproducibility. The subjective image quality analysis demonstrated >80% of segments are suitable for quantitative measurements, allowing regional measurements, which are

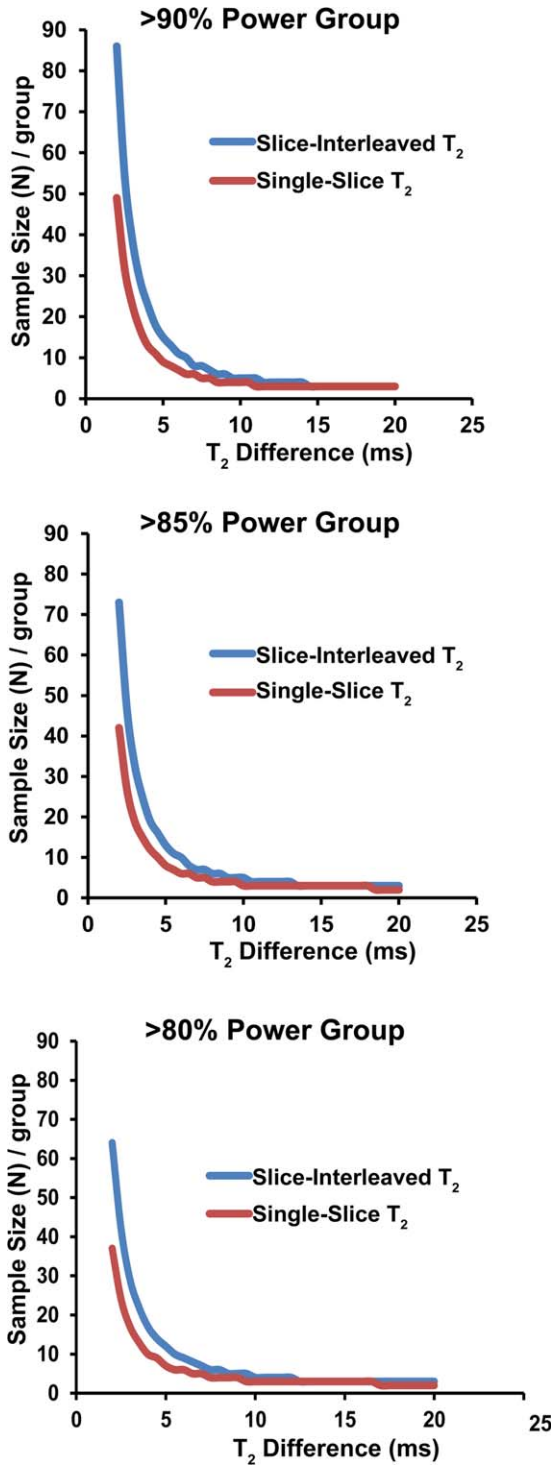

FIGURE 8: Assessment of required sample size for detection of corresponding T_2 differences in slice-interleaved T_2 and single-slice T_2 mapping sequences for three different power levels (>90%/ >85%/ >80%; $\alpha = 0.05$).

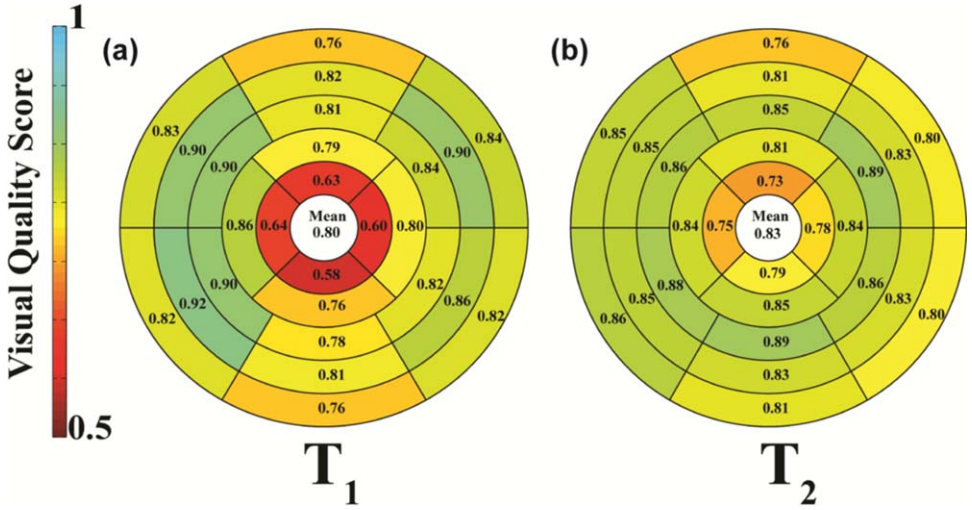

FIGURE 9: A 26-segment polar map of the left ventricle showing the average visual quality scores (0 = poor; 1 = good) for the two readers using the 26 segment LV model for T_1 mapping (a) and T_2 mapping (b), respectively.

important in certain diseases such as myocarditis and hypertrophic cardiomyopathy.

Our results expand on previous observations regarding the reproducibility of T_1 mapping using different T_1 mapping sequences.[18] While SASHA and SAPHIRE have excellent accuracy compared with MOLLI and ShMOLLI, they have lower reproducibility. The STONE sequence has a longer recovery time than MOLLI,[18,20] which improves accuracy and precision. Our data also support improved reproducibility of the STONE sequence as the coefficient of variation analysis for STONE was lower than similar studies with MOLLI.[26] There are very limited data on reproducibility for myocardial T_2 mapping.[27] In a test/retest study involving two separate days, Wassmuth et al[27] reported a high reproducibility of T_2 mapping with coefficients of variation from 6.6% to 7.6% depending on different imaging orientation.

Over the past several years, there have been significant advances in pulse sequence design for myocardial tissue characterization using T_1 and T_2 mapping. As we embark on the next challenge of using these sequences in larger clinical studies, we should incorporate measurement variability in power calculations for future studies. Our preliminary results demonstrated that the STONE T_1 sequence will lower the sample size needed to achieve a prespecified power to detect changes in T_1. In addition to advantages of reduced scan-time and free-breathing acquisition compared with other available T_1 mapping sequences, a lower sample size may reduce the overall cost of clinical studies and increase the sensitivity to detect smaller changes in T_1 in longitudinal studies. Our T_2 power calculation shows that similar numbers of patients are needed for the two sequences to detect expected T_2 differences; however, slice-interleaved T_2 will still require a shorter scan time. In our calculation, we did not consider nondiagnostic segments that should be accounted for when planning a clinical study to guarantee sufficient statistical power. Additional studies are warranted to calculate sample sizes in specific population of patients that might contain different degrees of T_1 and T_2 variability.

Our study has several limitations. The reproducibility measurements were only assessed in a small cohort of healthy young adult subjects and the statistical power analysis was mainly based on results in healthy subjects. The reproducibility may be lower in patients with different cardiovascular diseases. For example, in patients with dilated cardiomyopathy, the LV wall is often thin, making it difficult to measure T_1 or T_2 values. In our experience, it is difficult to perform similar test/retest studies on two separate days in patients; therefore, we only performed this study in healthy subjects. T_1 and T_2 may be dynamic. In our healthy cohort, we attributed the measurement variability to performance of the imaging sequence rather than to the changes in underlying T_1 or T_2. Nonetheless, this may not be the case in patients. We did not assess reproducibility of postcontrast T_1 or ECV in our healthy cohort as this would require contrast administration and hematocrit measurement. Additionally, we did not measure hematocrit in our patients, thus we only performed native T_1 sequence.

In conclusion, slice-interleaved T_1 and T_2 mapping yield highly reproducible myocardial T_1 and T_2 values, which may have implications for the determination of required sample sizes in larger clinical studies. Full LV coverage allows for assessment of various myocardial segments, with >80% for T_1 and >83% for T_2 maps of interpretable segments.

Acknowledgement

Contract grant sponsor: NIH; contract grant number: R01EB008743; R01HL129185-01; R21HL127650-01;

R01HL127015.; Contract grant sponsor: AHA; contract grant number: 15EIA22710040; Contract grant sponsor: Samsung Electronics

We thank Sophie Berg, RN; Kraig V. Kissinger, RT; Beth Goddu, RT; for patient recruitment and scanning and Gifty Addae for editorial assistance.

References

1. Dass S, Suttie JJ, Piechnik SK, et al. Myocardial tissue characterization using magnetic resonance noncontrast t1 mapping in hypertrophic and dilated cardiomyopathy. Circ Cardiovasc Imaging 2012;5:726–733.
2. Mewton N, Liu CY, Croisille P, Bluemke D, Lima JA. Assessment of myocardial fibrosis with cardiovascular magnetic resonance. J Am Coll Cardiol 2011;57:891–903.
3. Sparrow P, Messroghli DR, Reid S, Ridgway JP, Bainbridge G, Sivananthan MU. Myocardial T1 mapping for detection of left ventricular myocardial fibrosis in chronic aortic regurgitation: pilot study. AJR Am J Roentgenol 2006;187:W630–W635.
4. Thavendiranathan P, Walls M, Giri S, et al. Improved detection of myocardial involvement in acute inflammatory cardiomyopathies using T2 mapping. Circ Cardiovasc Imaging 2012;5:102–110.
5. Schelbert EB, Messroghli DR. State of the art: clinical applications of cardiac T1 mapping. Radiology 2016;278:658–676.
6. Moon JC, Messroghli DR, Kellman P, et al. Myocardial T1 mapping and extracellular volume quantification: a Society for Cardiovascular Magnetic Resonance (SCMR) and CMR Working Group of the European Society of Cardiology consensus statement. J Cardiovasc Magn Reson 2013;15:92.
7. Ugander M, Oki AJ, Hsu LY, et al. Extracellular volume imaging by magnetic resonance imaging provides insights into overt and subclinical myocardial pathology. Eur Heart J 2012;33:1268–1278.
8. Verhaert D, Thavendiranathan P, Giri S, et al. Direct T2 quantification of myocardial edema in acute ischemic injury. JACC Cardiovasc Imaging 2011;4:269–278.
9. Giri S, Chung YC, Merchant A, et al. T2 quantification for improved detection of myocardial edema. J Cardiovasc Magn Reson 2009;11:56.
10. Fitts M, Breton E, Kholmovski EG, et al. Arrhythmia insensitive rapid cardiac T1 mapping pulse sequence. Magn Reson Med 2013;70:1274–1282.
11. Mehta BB, Chen X, Bilchick KC, Salerno M, Epstein FH. Accelerated and navigator-gated look-locker imaging for cardiac t1 estimation (ANGIE): development and application to T1 mapping of the right ventricle. Magn Reson Med 2015;73:150–160.
12. Weingartner S, Akcakaya M, Roujol S, et al. Free-breathing combined three-dimensional phase sensitive late gadolinium enhancement and T1 mapping for myocardial tissue characterization. Magn Reson Med 2015;74:1032–1041.
13. Messroghli DR, Radjenovic A, Kozerke S, Higgins DM, Sivananthan MU, Ridgway JP. Modified Look-Locker inversion recovery (MOLLI) for high-resolution T1 mapping of the heart. Magn Reson Med 2004;52:141–146.
14. Piechnik SK, Ferreira VM, Dall'Armellina E, et al. Shortened Modified Look-Locker Inversion recovery (ShMOLLI) for clinical myocardial T1-mapping at 1.5 and 3 T within a 9 heartbeat breathhold. J Cardiovasc Magn Reson 2010;12:69.
15. Song T, Stainsby JA, Ho VB, Hood MN, Slavin GS. Flexible cardiac T1 mapping using a modified Look-Locker acquisition with saturation recovery. Magn Reson Med 2012;67:622–627.
16. Chow K, Flewitt JA, Green JD, Pagano JJ, Friedrich MG, Thompson RB. Saturation recovery single-shot acquisition (SASHA) for myocardial T mapping. Magn Reson Med 2014;71:2082–2095.
17. Slavin GS, Stainsby JA. True T1 mapping with SMART1Map (saturation method using adaptive recovery times for cardiac T1 mapping): a comparison with MOLLI. J Cardiovasc Magn Reson 2013;15(Suppl 1):P3.
18. Roujol S, Weingartner S, Foppa M, et al. Accuracy, precision, and reproducibility of four T1 mapping sequences: a head-to-head comparison of MOLLI, ShMOLLI, SASHA, and SAPPHIRE. Radiology 2014;272:683–689.
19. Weingartner S, Akcakaya M, Basha T, et al. Combined saturation/inversion recovery sequences for improved evaluation of scar and diffuse fibrosis in patients with arrhythmia or heart rate variability. Magn Reson Med 2014;71:1024–1034.
20. Weingartner S, Roujol S, Akcakaya M, Basha TA, Nezafat R. Free-breathing multislice native myocardial T mapping using the slice-interleaved T (STONE) sequence. Magn Reson Med 2014;74:115–124.
21. Huang TY, Liu YJ, Stemmer A, Poncelet BP. T2 measurement of the human myocardium using a T2-prepared transient-state TrueFISP sequence. Magn Reson Med 2007;57:960–966.
22. van Heeswijk RB, Piccini D, Feliciano H, Hullin R, Schwitter J, Stuber M. Self-navigated isotropic three-dimensional cardiac T2 mapping. Magn Reson Med 2015;73:1549–1554.
23. Basha TA, Bellm S, Roujol S, Kato S, Nezafat R. Free-breathing slice-interleaved myocardial T2 mapping with slice-selective T2 magnetization preparation. Magn Reson Med 2015. doi: 10.1002/mrm.25907 [Epub ahead of print].
24. Roujol S, Foppa M, Weingartner S, Manning WJ, Nezafat R. Adaptive registration of varying contrast-weighted images for improved tissue characterization (ARCTIC): application to T1 mapping. Magn Reson Med 2015;73:1469–1482.
25. Akcakaya M, Basha TA, Weingartner S, Roujol S, Berg S, Nezafat R. Improved quantitative myocardial T2 mapping: impact of the fitting model. Magn Reson Med 2014;74:93–105.
26. Messroghli DR, Plein S, Higgins DM, et al. Human myocardium: single-breath-hold MR T1 mapping with high spatial resolution--reproducibility study. Radiology 2006;238:1004–1012.
27. Wassmuth R, Prothmann M, Utz W, et al. Variability and homogeneity of cardiovascular magnetic resonance myocardial T2-mapping in volunteers compared to patients with edema. J Cardiovasc Magn Reson 2013;15:27.